Electronic supplementary information

Cells function as a ternary logic gate to decide migration direction under integrated chemical and fluidic cues

Hye-ran Moon, [a] Soutick Saha, [b] Andrew Mugler,[bcd] and Bumsoo Han [*ace]

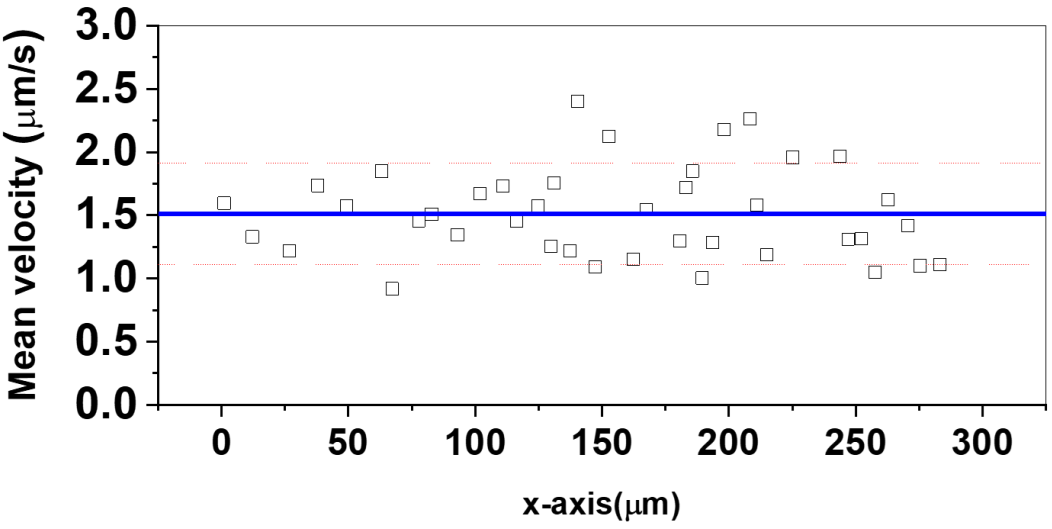

Figure S1. Flow velocity simulated by fluorescent polystyrene beads of 0.2μm diameter. Dot: The velocity of the collected particles distributed along with the x-locations. Blue line indicates average of all collected particles' velocity and red dash lines indicate standard error.

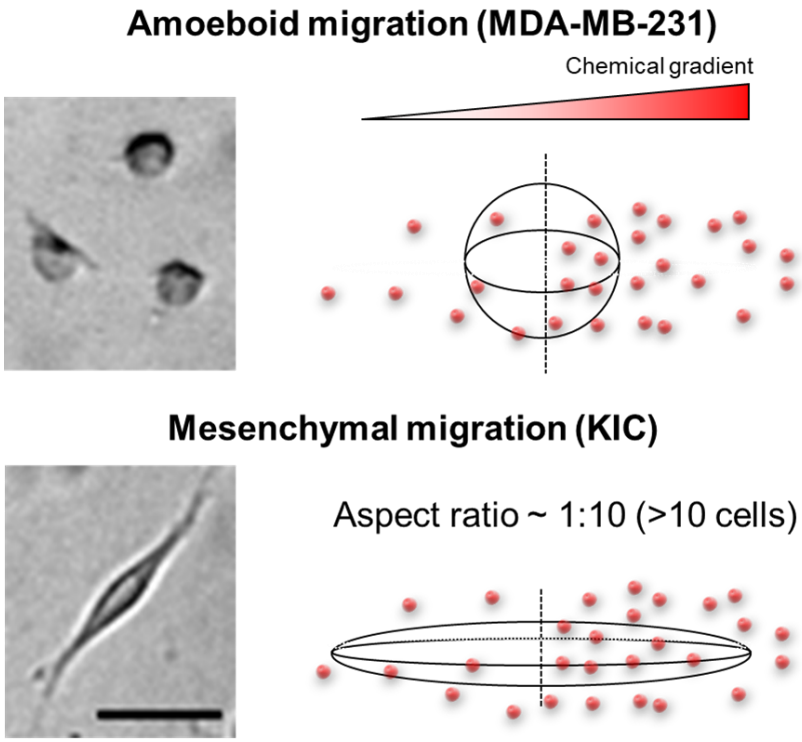

$$S = \frac{\text{Surface area of ellipsoid (mesenchymal)}}{\text{Surface area of sphere}}$$

Figure S2. Shape factor to adjust the mesenchymal morphology of KIC cells in relative gradient of the chemical concentration across the cell body (γ) .

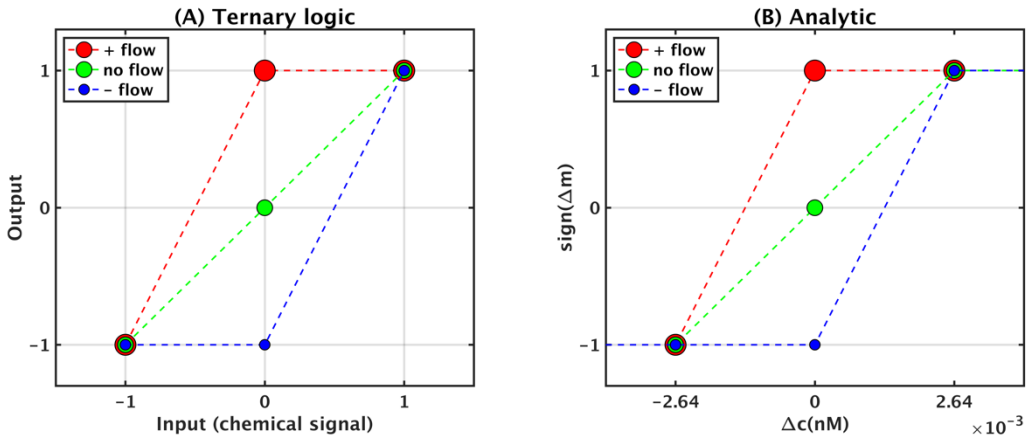

Figure S3. Relationship between ternary logic gate model and analytic expression for Δm

There is a one-to-one correspondence between the (A) ternary logic gate model as shown in Figure 5 analytic expression for Δm in Eq. 3. The expression of the output (*Y*) in Figure 5 can be written as $Y = (f(1 - |g|) + g) \times (1 - \bar{c})$, where $g = 1$ if ΔTGF is positive and above the detection limit, $g = 0$ if ΔTGF is below the detection limit or absent, and $g = -1$ if ΔTGF is negative and above the detection limit;; $f = 1$ if the pressure gradient is positive (such that the flow is in the negative direction and cells would move in the positive direction upstream), $f = 0$ if flow is absent, and $f = -1$ if the pressure gradient is negative; and $\bar{c} = 1$ if the background TGF concentration is above the saturation limit (~10 nM as indicated in Figure 4D), and $\bar{c} = 0$ if the background TGF concentration is below the saturation limit.. In A, the vertical axis is Y, the horizontal axis is g, the legend indicates f, and $\bar{c} = 0$. In B, the sign of Eq. 3 is plotted with the parameters fitted in the main text, where 2.64×10^{-3} nM is the concentration at which Δm changes sign in the presence of flow. In both cases, we see that the output only reflects the flow state if the chemical gradient is absent (A) or sufficiently small (B).

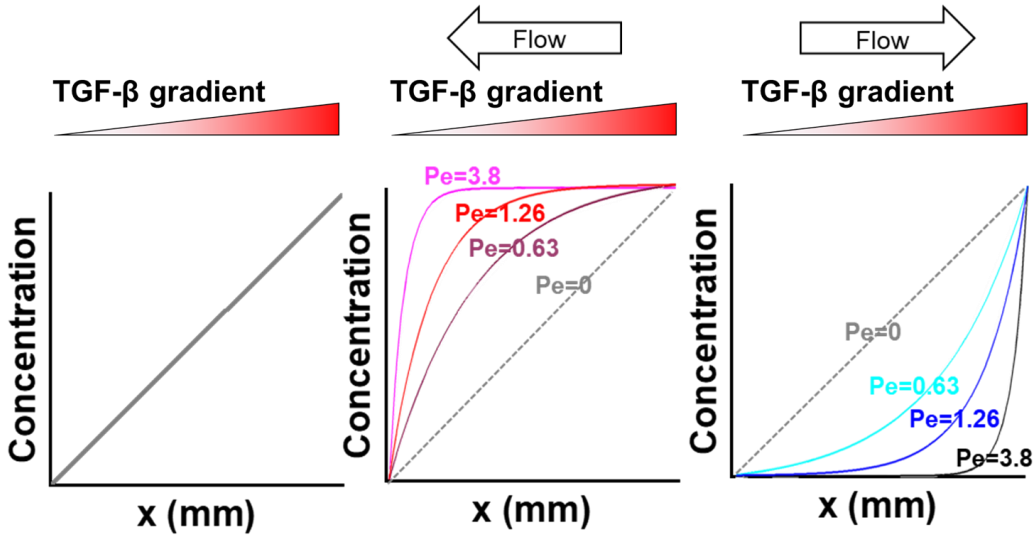

Figure S4. Concentration profiles of the chemical cue integrated with fluidic cue with various Pe numbers (Pe=0, 0.63, 1.26, and 3.8) for each flow condition of (A) no-flow, (B) parallel flow, and (C) counter flow.

Physical model- shared pathway model

The dynamics of x, y, b and m from the network in **Fig. 4A** are given by,

$$\dot{x} = k_1 c - k_2 x$$

$$\dot{y} = k_3 f - k_4 y$$

$$\dot{b} = \left(k_5 + k_6 x + k_7 y\right)\left(b_0 - b\right) - k_8 b$$

$$\dot{m} = k_9 b - k_{10} m$$

Where b_0 is the total amount of molecules of type A and B. k_is are rates of reactions, c is the external chemical concentration and f is the corresponding effect due to the flow. The underlying assumption of putting f and c in the same footing is that both the chemical signal and flow activates internal molecules X and Y in the cell. The steady state expression of m is,

$$m = \frac{k_9}{k_{10}} \frac{\left[k_5 + \left(\frac{k_6 k_1}{k_2}\right) c + \left(\frac{k_7 k_3}{k_4}\right) f\right] b_0}{k_5 + k_8 + \left(\frac{k_6 k_1}{k_2}\right) c + \left(\frac{k_7 k_3}{k_4}\right) f}$$

To determine the difference of m between two halves of the cell we use,

$$\Delta m \cong \frac{\partial m}{\partial c} \Delta c + \frac{\partial m}{\partial f} \Delta f$$

Where the first term is the contribution due to the chemical gradient and the second term is the contribution due to the flow. Simple algebra leads to the expression,

$$\Delta m = \frac{k_8 k_9 b_0}{k_{10}\left(k_5 + k_8\right)^2} \frac{\left[\left(\frac{k_6 k_1}{k_2}\right) \Delta c + \left(\frac{k_7 k_3}{k_4}\right) \Delta f\right]}{\left[1 + \left(\frac{k_6 k_1}{k_2\left(k_5 + k_8\right)}\right) \bar{c} + \left(\frac{k_7 k_3}{k_4\left(k_5 + k_8\right)}\right) f\right]^2}$$

Where $\bar{c}$ is the background chemical concentration and Δc is the difference of chemical molecules between two halves of the cell and f and Δf are the corresponding effect due to

the flow. $\bar{c}$ and Δc can be rewritten in terms of known quantities as $a'g$ where a' is the cell length and g is the chemical gradient.

We can also define the following parameters,

$$m_0 = \frac{k_9 b_0}{k_{10}};\ \mu = \frac{k_5}{k_5 + k_8};\ \beta_c = \frac{k_6 k_1}{k_2(k_5 + k_8)};\ \beta_f = \frac{k_7 k_3}{k_4(k_5 + k_8)}$$

Where m_0 represents a concentration scale, μ is a dimensionless ratio for b reaction, and β_i can be understood as a reaction efficiency from the cue to m. If β_i is larger, faster reaction rates and slower dissociation rates for the specific pathway to convert m. (i.e. β_c ↑ when k_1 ↑, k_6 ↑ and k_2 ↓) To get the expression in Eq.3 in the main text,

$$\Delta m = m_0(1-\mu)\frac{\beta_c g a' + \beta_f \Delta f}{(1 + \beta_c \bar{c} + \beta_f f)^2}$$

Here, we can define dimensionless parameters, implying "amplification factor" (η_i), including a reaction efficiency and signal strength.

$$\eta_c = \beta_c \bar{c},\ \ \eta_f = \beta_f f$$

Now observations from our own cancer cell migration experiments suggest there is always a random component to migration (mean and median DAI is always less than the maximum possible value 1). Moreover, DAI is bounded between -1 and 1 and Δm is unbounded. So, to draw a more direct analogy of Δm to DAI we define the probability distribution of migration angles θ as a function of Δm as a biased random walk model [1]

$$p(\theta) = \frac{1-\alpha}{2\pi} + \frac{\alpha e^{-(\Delta m)\cos\theta}}{2\pi I_0(\Delta m)}.$$

Where, $0 \le \alpha \le 1$ is the maximum possible mean DAI ($\langle DAI \int_0^{2\pi} cos(\theta)\, p(\theta) d\theta \rangle$=) and I_0 is the modified Bessel function of the first kind. The value of Δm suggests how close mean DAI is to α. The larger and positive Δm is the closer mean DAI is to α and as $\Delta m \to \infty, \langle \mathrm{DAI} \rangle \to \alpha$.

Now we set $\alpha, m_0, \mu, \beta, \phi(=\beta_f \Delta f)$, and $\eta_f(=\beta_f f)$ are the unknown parameters. Among these we set α equal to the maximum mean DAI in experiments in **Fig. 4C**. The other four unknown parameters are set to give minimum total absolute error between the experimental median DAI and median DAI using our model in experiments shown in **Fig. 4C**. The best set of parameter values are,

$$m_0(1-\mu) = 3003.9; \beta_c = 0.9073; \phi = 0.0018; \eta_f = 1.6612.$$

Analogy between cellular selection of a specific cue direction and signal processing through the shared pathway model.

We can define the relative gradient of each cue across the cell body, which could indicate the extracellular cue strength.

$$\gamma_c = \frac{\Delta c}{\bar{c}}, \ \gamma_f = \frac{\Delta f}{f}$$

Then Δm can be represented as:

$$\Delta m = m_0(1-\mu)\frac{\gamma_c\eta_c + \gamma_f\eta_f}{(1+\eta_c+\eta_f)^2}$$

The difference of molecule m (Δm) corresponding to the cellular directional accuracy can be dependent on the cell type (μ), extracellular strength for each cue (γ) and each cue's amplification ability through the signaling pathway (η). We define the relative extracellular cue strength and the relative intracellular pathway strength to get an expression in Eq.5.

In the experiment, we observed that cells select a chemical cue to follow in their movement direction, specifically when the counter flow was applied. Based on this understanding, we developed rationales for how the cells can preferentially select a specific cue (in our results, chemical cue to fluidic cue) with the sign of Δm.

$$\frac{\Delta m}{m_0} = (1-\mu)\frac{\gamma_c\eta_c(1+\varepsilon\rho)}{(1+\eta_c+\eta_f)^2}$$

Where the relative fluidic cue strength ε is defined as γ_f / γ_c, and the relative fluidic pathway strength $\rho = \eta_f / \eta_c$. The counter flow can be described with negative ε ($\gamma_f < 0$ and $\gamma_c > 0$) where pathway strength is always positive ($\rho > 0$). We define the cellular section of the

chemical cue when Δm>0, whereas the selection of the fluidic cue when Δm<0. Consequently, the sign of Δm is determined by $(1+\varepsilon\rho)$.

We can also consider the total cue strength and pathway strength, ($\omega = \gamma_c + \gamma_f$ and $\psi = \eta_c + \eta_f$, respectively). Then, the equation converted to the following form:

$$\frac{\Delta m}{m_0} = (1-\mu)\frac{\omega\psi(1+\varepsilon\rho)}{(1+\rho)(1+\varepsilon)(1+\psi)^2}$$

Where $\omega=\gamma_c(1+\varepsilon)$, below conditions are satisfied in any case.

$$\rho > 0,\ \psi > 0$$

$$\frac{\omega\psi}{(1+\rho)(1+\varepsilon)(1+\psi)^2} > 0$$

Consequently, the sign of Δm is determined by $(1+\varepsilon\rho)$ regardless of ω and ψ.

As we represented in **Fig. 6**, ε can be bounded depending on the physiologically possible strength range of the cues. Specifically, we have analyzed that the fluidic cue can vary the chemical gradient profile. In that sense, the chemical cue strength (γ_c) and fluidic cue strength (γ_f) are dependent. When the flow velocity increases, the chemical gradient strength is intuitively expected to decrease. However, the chemical cue strength defined as a relative gradient across the cell body is larger than 1% since cells only can capture the shallow gradient over γ_c=1%. Therefore, the minimum possible γ_c can be 0.01. The physiological range of the flow velocity has been reported as tissue-dependent. In the tumor microenvironment, the flow velocity is in the low Reynolds number range of 0.5–4μm/s [2-4].

The fluidic cue is relevant to the interstitial flow velocity over the cell surface [5]. Although it has still been elusive how the cells can sense the fluidic cue, we assume that the fluidic cue strength is linearly proportional to the interstitial flow velocity. Here we do not consider the

autologous chemotaxis by the flow. The proposed model estimated γ_f as 0.0011. Then the relative fluidic cue strength (ε) is physiologically possible in the range:

$$|\varepsilon| < 0.29$$

In the range, the cells have a higher chance of preferentially selecting the chemical cue in their migration direction (**Fig. 6**).

References

1. J. Varennes, H.-r. Moon, S. Saha, A. Mugler and B. Han, *PLOS Computational Biology*, 2019, **15**, e1006961.
2. G. Follain, D. Herrmann, S. Harlepp, V. Hyenne, N. Osmani, S. C. Warren, P. Timpson and J. G. Goetz, *Nature Reviews Cancer*, 2020, **20**, 107-124.
3. M. A. Swartz and M. E. Fleury, *Annual review of biomedical engineering*, 2007, **9**, 229-256.
4. M. A. Swartz, N. Iida, E. W. Roberts, S. Sangaletti, M. H. Wong, F. E. Yull, L. M. Coussens and Y. A. DeClerck, *Cancer Research*, 2012, **72**, 2473-2480.
5. W. J. Polacheck, J. L. Charest and R. D. Kamm, *Proceedings of the National Academy of Sciences*, 2011, **108**, 11115-11120.